A Radar-Based Breast Cancer Detection System Using CMOS Integrated Circuits

**HANG SONG[1], HAYATO KONO[1], YUJI SEO[1], AFREEN AZHARI[1], JUNICHI SOMEI[2],
EIJI SUEMATSU[2], YUICHI WATARAI[2], TOSHIHIKO OTA[3], HIROMASA WATANABE[3],
YOSHINORI HIRAMATSU[3], AKIHIRO TOYA[4], XIA XIAO[5], (Member, IEEE),
AND TAKAMARO KIKKAWA[1], (Fellow, IEEE)**

[1]Research Institute for Nanodevice and Bio Systems, Hiroshima University, Higashi-hiroshima 739-8527, Japan
[2]Sharp Corporation, Fukuyama 721-8522, Japan
[3]Sharp Takaya Electronic Industry Company, Ltd., Yakage 714-1211, Japan
[4]Kure National College of Technology, Kure 737-8506, Japan
[5]School of Electronic and Information Engineering, Tianjin University, Tianjin 300072, China

Corresponding author: T. Kikkawa (kikkawat@hiroshima-u.ac.jp)

ABSTRACT An ultrawideband (UWB) radar-based breast cancer detection system, which is composed of complementary metal–oxide–semiconductor integrated circuits, is presented. This system includes Gaussian monocycle pulse (GMP) generation circuits, switching (SW) matrix circuits, equivalent-time sampling circuits, and a compact UWB antenna array. During the detection process, the GMP signal with the center frequency of 6 GHz is first generated and transmitted with a repetition frequency of 100 MHz. The GMP signal is sent to a selected transmitter antenna by the SW matrix module, and the reflected signal is captured by the receiver antennas. Next, the high-speed equivalent-time sampling circuits are employed to retrieve the reflected GMP signal. A confocal algorithm is used to reconstruct the breast image. The total size for the prototype module is 45 cm × 30 cm × 14.5 cm in length, width, and height, respectively, which is dramatically smaller than the conventional detection systems. Using our proposed system, we demonstrate a successful detection of 1-cm cancer target in the breast phantom.

INDEX TERMS Breast cancer, CMOS, microwave imaging, ultrawideband, confocal algorithm.

I. INTRODUCTION

To date, the most commonly used method for breast screening is mammography because it has a relatively high accuracy. However, there are some drawbacks such as exposure to ionizing radiation and compressing of breast which will make the patients feel uncomfortable. What is even worse is that the ionizing radiation will increase the probability of getting cancer, resulting in the limitation of the frequent use [1].

To overcome the shortage of the existing method, some complementary methods have been proposed and studied such as the electrical impedance tomography (EIT) and microwave imaging. The EIT method exploits very low frequency wave to draw the conductivity distribution of the breast [2]–[5]. The microwave imaging employs the high frequency wave. This method is based on the difference in the dielectric properties between the normal breast tissues and cancer tissues [6]–[8]. At present, many research groups which are devoted to develop microwave imaging [9]–[21].

Some groups focus on the microwave sensors and hardware components [22]–[24]. However the entire system has not been developed. Some groups have developed many useful signal processing and imaging algorithms but most of these are studied in simulation cases [25]–[28].

There are groups who have developed the prototype detection systems, which reflect the state of the art in microwave imaging [29]. Generally, there are two microwave imaging methods regarding to the waveforms. One is called the radar-based approach where the ultrawideband (UWB) signal is used. Klemm and Craddock *et al.* have proposed a multi-static radar-based detection system, where they fixed the antenna array by using a hemispherical antenna dome [30], [31]. This system requires the woman to lie in prone position and making the breast pendant into the dome. The antennas are excited in turn and reflections are collected by the other ones. This experiment is conducted by using of a VNA and bank switches. Fear *et al.* have proposed a mono-static

radar-based system, where only one Vivaldi antenna is used to both emit and receive signals [32], [33]. By changing the position of the antenna, all necessary data set can be collected and used to generate the breast image. This system uses the VNA to transmit and receive the signal and a tank with matching liquid media is employed where the breast is immersed. Both of the mentioned systems use the delay and sum approach in the imaging process. The other mostly studied approach is called microwave tomography, where multi-frequencies are used to reconstruct the whole distribution of the breast dielectric property [34]–[36]. Meaney et al. have developed a 3D parallel-detection system with 16 vertically-oriented monopole array antennas [37]. This system uses signal generator to transmit continuous single frequency signal. A 3D iterative Gauss-Newton algorithm is utilized to reconstruct the dielectric distribution in the breast. All the aforementioned systems have achieved some good results of detecting the breast tumor in clinical use. However, these systems are established by large and relatively expensive commercial equipments.

For the purpose of frequent use of microwave imaging, by which women can conduct self-examination at home, the miniaturization and reasonable price of the detection system is highly desired. To achieve this goal, the complementary metal-oxide-semiconductor (CMOS) integrated circuits are developed to be able to replace the large equipment.

In this paper, a detection system is developed by use of CMOS circuits. To the best of our knowledge, this is the first complete breast cancer detection system using CMOS circuits. This system does not need any off-the-shelf large and expensive equipment. In this system, a UWB signal generation circuits can generate and transmit the monocycle Gaussian pulse without any transformation [38], [39]. The switching (SW) matrix circuits can choose the signal channel to excite the UWB antenna array in turn [40]. The equivalent time high-speed sampling circuits can sample and digitalize the received signals [41], [42]. Then the digitalized signals are stored into the PC for post-processing to generate the breast image. This paper is organized as follows. Section II describes the composition of the system. Section III presents the detection experiment setup to obtain the signals. Section IV presents the confocal imaging results using different signals and different artifact removal methods. Finally, a conclusion is declared in the last section.

II. HARDWARE COMPOSITION

The proposed system is comprised of several functional modules. Among these, the key parts are the UWB signal generation module, switching matrix module and the receiver module. To control and coordinate these functional parts, a control board is developed and consolidated into a box. Meanwhile, the graphic user interface (GUI) software is developed to let users adjust the output of the control board. The essential components and the integrated system are described in the following sections.

A. TRANSMITTER MODULE

The concept about the generation of the UWB signal is to combine the up and down slopes of the input signals to form a Gaussian monocycle pulse (GMP). The entire schematic diagram of differential GMP generator circuit is illustrated in Fig. 1 [43]. The input clock and the data are transmitted through some logic circuits and delay circuits and then the GMP is generated.
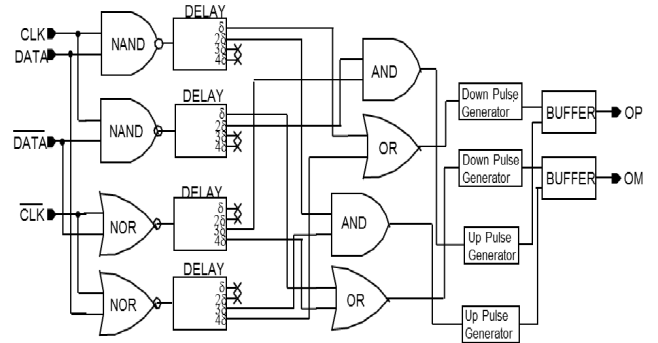

FIGURE 1. Block diagram of GMP signal generator module.

To form the GMP pulse, the up-pulse and down-pulse should be generated separately. The relevant schematic diagrams are detailed in Reference [44].

The output signals are shown in Fig. 2. The pulse width is about 160 ps and the center frequency is about 6 GHz. In implementation, a 100 MHz frequency clock is inputted into the module and the output signals from OP and OM are the differential GMP trains with the repetition frequency of 100 MHz.
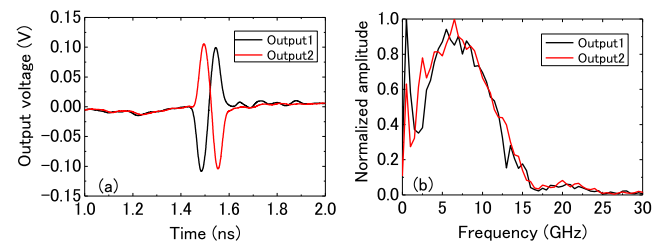

FIGURE 2. The differential output GMP signals of the transmitter module in time domain and frequency domain. (a) Time domain. (b) Frequency domain.

B. SWITCHING MATRIX

This system is designed with the ability to transmit and receive signals through 16 antennas, among which 8 antennas are designated as transmitters and the other 8 antennas are designated as receivers. To change the operating antenna pair, a switching module is necessary. In our system, a single pole eight throw (1P8T) switching matrix module is developed and two separate modules are employed to select the transmitter antennas and the receiver counterparts, respectively. The schematic diagram of the switching matrix is shown in Fig. 3 [40].
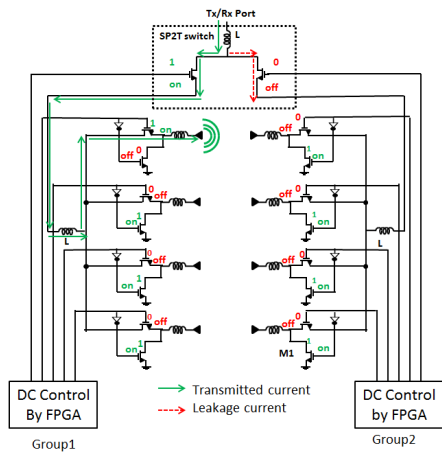
FIGURE 3. Schematic circuit diagram of 1P8T switching matrix.

The input signal is transmitted to Tx port through the SMA connector. A control board is developed to control the switching matrix module and then the path to be used is chosen to transmit and excite the corresponding antenna. The switching matrix circuit is assembled by the flip-chip bonding to the PCB and the 8 mini-SMP connectors are mounted to connect with the antennas.

A 4×4 planar UWB antenna array serves as the transmitter and receiver of the signal [45]. The connection between the antenna array and switching matrix is shown in Fig. 4. The antenna 1∼4 and 9∼12 servers as the transmitters (Tx) and the antenna 5∼8 and 13∼16 serves as the receivers (Rx).
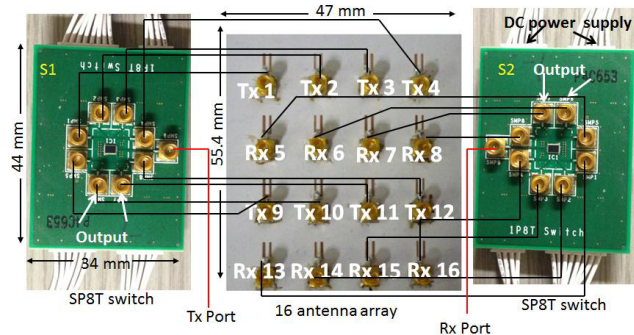

FIGURE 4. Photographs of switching matrix module and the antenna array.

C. RECEIVER MODULE

To receive and record the reflected signal from the breast, whose duration is very short, a high-speed sampling circuit is necessary. However it is difficult to sample the signals with the speed of tens GHz by CMOS technology. We have developed a high-speed equivalent time sampling circuits [41], [42]. This is realized based on the fact that our system is operated at a repetition frequency of 100 MHz. Therefore, the received GMP signal train is also repetitive and the sampling timing can be at different period of the

received signal with a precise phase difference. The concept of this sampling structure is explained in this section. The conceptual graph and schematic diagram is shown in Fig. 5.
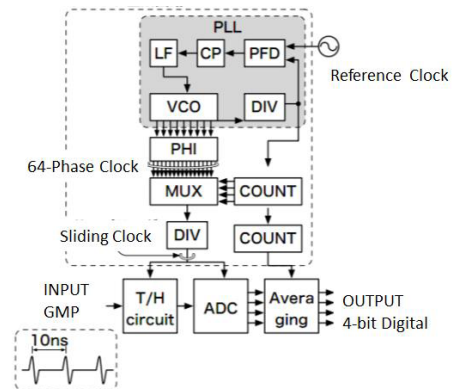

FIGURE 5. Block diagram of equivalent time sampling circuits.

The sampling module generates a 16-phase 1.6 GHz shifting clock by a phase lock loop (PLL) with an 8-stage ring-voltage control oscillator (VCO) of 1.6 GHz oscillation frequency with the reference clock of 100 MHz. Then, a two-stage phase interpolator (PHI) is employed to further improve the resolution of the clock, which makes the clock have 64 phases in one period. This means 64 samples can be obtained in duration of 0.625 ns. Eventually, a sampling clock which has a phase shift resolution of 9.77 ps is obtained. Using this clock with a 9.77 ps shift in each 10 ns period to control the track and hold (T/H) circuit and analog-to-digital (ADC) circuit, the equivalent time sampling rate of 102.4 GS/s is achieved. Figure 6 shows the simulation results of the T/H circuit. It can be seen that the input signal is sampled in a slow mode and the duration of output signal is about 1000 times of the original one.
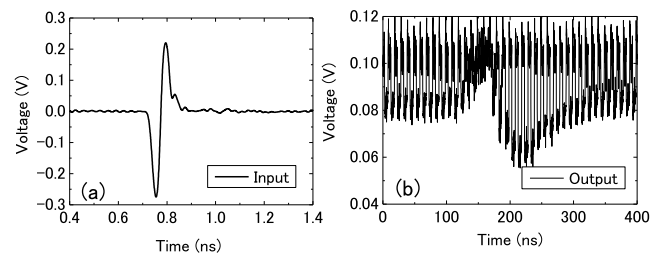

FIGURE 6. The simulation results of the T/H circuit. (a) Input signal. (b) Output signal.

At present, the accuracy of the ADC is 4-bit and the range covered can be changed from 0V to 1.4V.

D. INTEGRATED SYSTEM DESIGN

The complete breast cancer detection system is integrated by combing the essential function modules, amplifier parts, antenna array and the control board. The block diagram of the system is shown in Fig. 7.
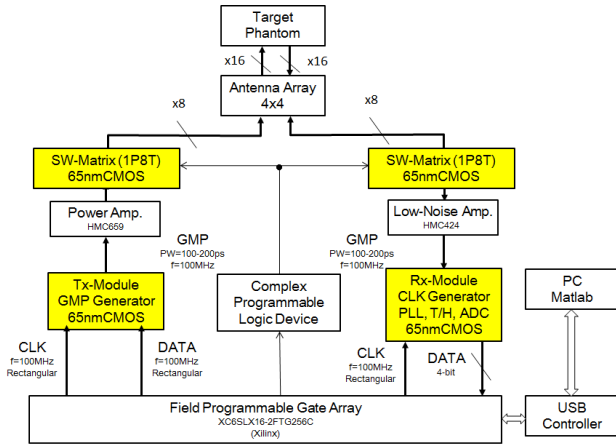
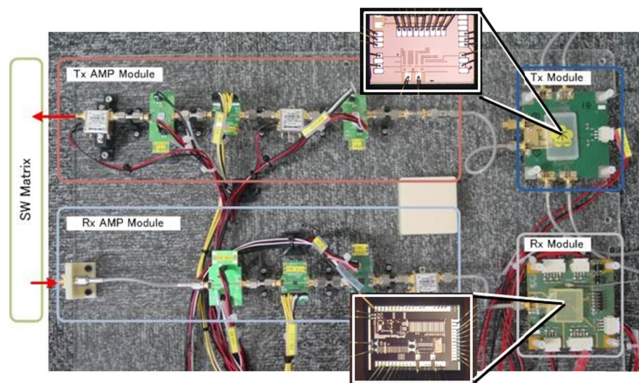**FIGURE 7.** Block diagram of breast cancer detection system.

FIGURE 8. Photograph of the functional parts of the detection system.

Figure 8 shows the functional parts of the system. The Tx Amp. module consists of a DC cut (ST159-0002-000, Sharp Takaya Electronic Industry), a fixed attenuator (BW-S3W2+, Mini-circuits), two power amplifier (HMC659LC5, Hittite Microwave Corporation) and a step attenuator (HMC424LP3, Hittite Microwave Corporation). The operation frequency range of this module is from 2 GHz to 12 GHz. The total size of the Tx amp module is about 300 mm × 50 mm × 35 mm. As the reflected signal is weak, an Rx AMP module is configured between the receiver and Rx module. This module consists of two LNAs (HMC424LP3 and HMC1049LP5, Hittite Microwave Corporation), a step attenuator (HMC424LP3, Hittite Microwave Corporation) and a DC cut (ST159-0002-000, Sharp Takaya Electronic Industry). The operation frequency is 2 GHz to 12 GHz. The total size of the Rx AMP module is 200 mm × 50 mm × 40 mm.

A control board is developed to coordinate the operation of the system. The control board is connected with the PC through a UWB port and GUI software is developed to give command to the whole system. The power supply of the control board is 12V DC from an adaptor and the power supply block provides power to all other parts with corresponding voltages. The reference voltages for ADC can be

adjusted by the software. The clock generator block feeds the inputs (DATA, $\overline{\text{DATA}}$, CLK, $\overline{\text{CLK}}$) to the Tx module. The digital & RF control block manages the gain of amplifiers and attenuators to regulate the output amplitude of the system. Meanwhile, it stores and sends the digitalized data to the PC for post-processing. The photo of the entire system is shown in Fig. 9.
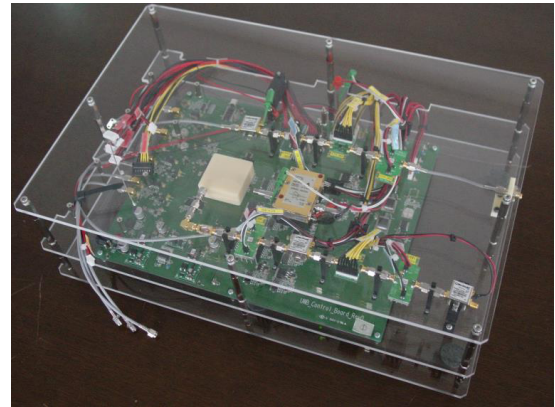

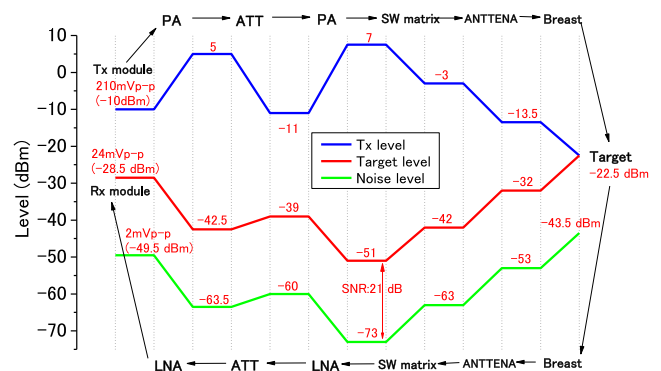**FIGURE 9.** Photograph of the entire system.

FIGURE 10. The level diagram of the system.

The level diagram of the system is shown is Fig. 10. The peak-to-peak amplitude of the GMP signal from Tx module is 210 mV which is about −10dBm. The input signal goes through the amplifier and SW matrix and emitted by the antenna array. The amplitude of the emitted signal is −13.5 dBm. As the signal is generated with a period of 10 ns and the duration of each pulse is 160 ps, the duty of the signal is 1.6%. Therefore, the actual emission power is −31.5 dBm. The bandwidth of the signal is about 6.7 GHz and then the emission level is −69.5 dBm/MHz which is lower than the FCC regulation for UWB (−41.25 dBm/MHz). The system noise (kTB+NF) for the LNA is calculated by the equations,

$$kTB = 1.38 \times 10^{-23} \times 309.15 \times 6.7 \text{ GHz}$$
$$= 28 \times 10^{-9} \text{ mW} = -75.44 \text{ dBm} \quad (1)$$
$$\text{Noise Level} = kTB + NF = -75.44 \text{ dBm} + 2.5 \text{ dBm}$$
$$= -73 \text{ dBm} \quad (2)$$

where k is Boltsmann constant, T is the human body temperature, B is the bandwidth of the signal and NF is noise figure, respectively.

III. DATA ACQUISITION

A. BREAST PHANTOM AND EXPERIMENT SETUP

In order to demonstrate the performance of the developed system, a homogeneous breast phantom is used in this experiment. Bacon with the size of 10 mm × 10 mm × 10 mm is placed at the depth of 20 mm below the antenna array as a target. The breast phantom is made of rubber and the total size is 15 cm × 15 cm × 4 cm. The dielectric properties of the rubber are similar to those of the fatty tissue. The bacon also has similar properties to those of the tumor tissue. The measured dielectric properties of rubber, bacon, fatty tissue and tumor are shown in the Fig. 11.
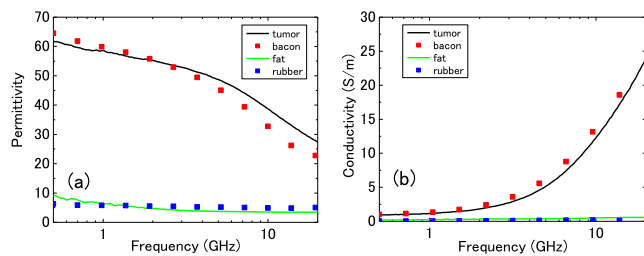
FIGURE 11. The measured dielectric properties of bacon, tumor, rubber and fatty tissues. (a) Permittivity. (b) Conductivity.

The detection system is connected to the antenna array by 16 cables and the antenna array is placed on the breast phantom as shown in Fig. 12.
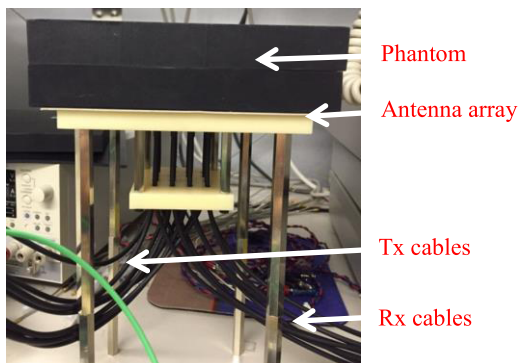
FIGURE 12. Breast phantom and experiment settings.

B. MEASURED WAVEFORMS

During the experiment, the Tx antennas are excited in turn and the reflected signals are captured by the Rx antennas. The receiving signals are then amplified and sampled by the Rx module. For the experiment case in this article, the reference voltages of the ADC are chosen as 330 mV and 690 mV, respectively. Thus the LSB is 22.5 mV. Figure 13 shows the measured signals by some antenna pairs.
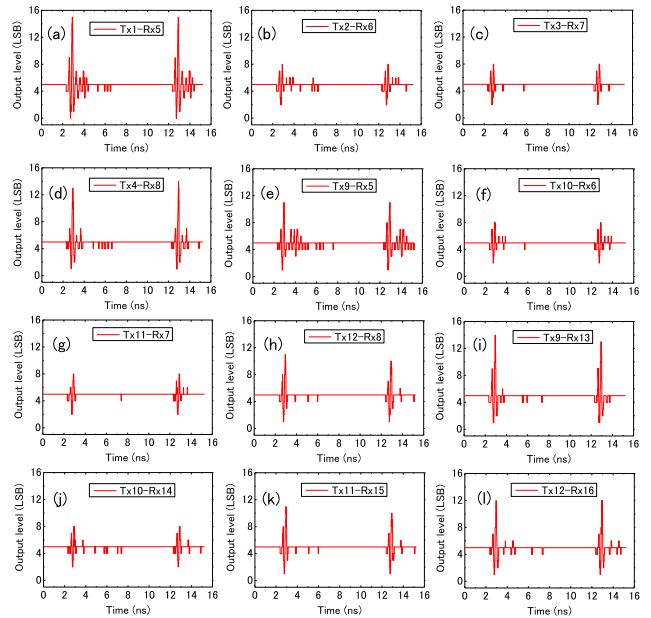
FIGURE 13. The measured digitalized signals from different Tx and Rx antenna pairs. (a) Tx1-Rx5. (b) Tx2-Rx6. (c) Tx3-Rx7. (d) Tx4-Rx8. (e) Tx9-Rx5. (f) Tx10-Rx6. (g) Tx11-Rx7. (h) Tx12-Rx8. (i) Tx9-Rx13. (j) Tx10-Rx14. (k) Tx11-Rx15. (l) Tx12-Rx16.

IV. IMAGE RECONSTRUCTION

To extract the tumor response from the raw data, the artifacts which contain early reflections and direct waves should be removed. There are many artifacts removal algorithms [46]–[48]. For the ideal case, detection is carried out with the tumor-free breast phantom to get the reference signals and then subtract reference signals from raw data. This method is not practical in clinical case. However, we can use it as a preliminary way to test the performance of the entire system. Meanwhile, it can be regarded as a criterion to evaluate other algorithms. In this section, both ideal and averaging algorithms are used to remove the artifacts and the imaging results are presented.

A. IMAGING FROM RAW DATA

In this case, the ideal artifact removal algorithm is used. As there are some vibrations caused by physical movement or temperature change between the original and reference experiments, offsets sometimes exist between the two kinds of received signals. Figure 14 shows the sampled 4-bit digital signals which is emitted by transmitter antenna 1 (Tx1) and received by receiver antenna 5 (Rx5). It is can be seen that the offset exists. As shown in Fig. 15, the offsets also can be observed in other antenna pairs such as Tx1-Rx6 and Tx10-Rx6. Thus, it is necessary to align the sampled signals in the two experiments.

The concept of the alignment is to adjust the peaks of the signals. However, it is difficult to recognize the signal peak in some antenna pairs. Figure 16 shows some examples of the signals where the peaks cannot be confirmed. This is caused
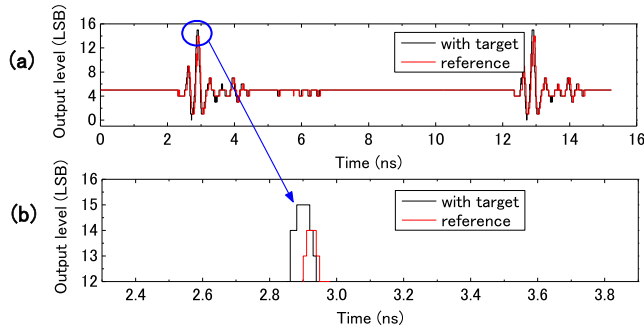
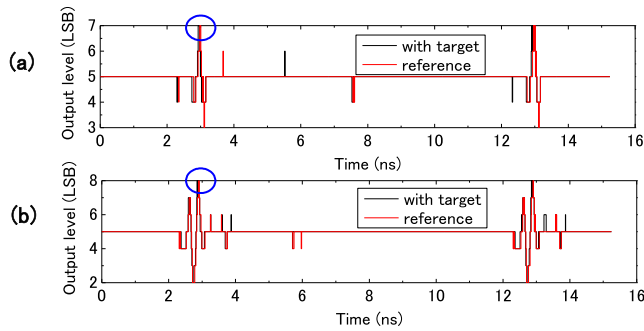**FIGURE 14.** Digital signals from antenna pair Tx1-Rx5. (a) Time-domain sampled waveforms. (b) Enlarged.

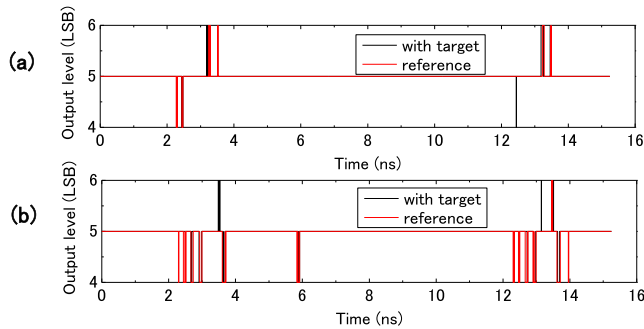**FIGURE 15.** The sampled digital signals. (a) Tx1-Rx6. (b) Tx10-Rx6.

FIGURE 16. The sampled digital signals. (a) Tx4-Rx14. (b) Tx9-Rx16.

by the accuracy of the ADC. As the signals in some antenna pairs are very weak, the 4-bit ADC failed to differentiate them. Since the alignment cannot be done in the cases where the signal peak cannot be found and the subtracted signals may be only noise, the signals from these antenna pairs are ignored in the following processing procedure and confocal imaging. Contrarily, the signals where the peak can be recognized are chosen.

To correct the offset in 'with target' and 'reference' signals, the signal adjustment procedure is carried out. The procedure of the adjustment is as follows, for each selected signal in turn:

1. Find the first continuous peaks of the received signal when tumor exists. And then calculate the average time of the peaks t_1.
2. Find the first continuous peaks of the received signal when tumor doesn't exist. And then calculate the average time of the peaks t_2.

3. Calculate the offset between the two signal peak time:

$$dt = t_1 - t_2 \qquad (3)$$

4. Offset the 'reference' signal S_{ref} to match the 'with target' signal and set the new 'reference' signal as:

$$S_{ref\_new}(t) = S_{ref}(t + dt) \qquad (4)$$

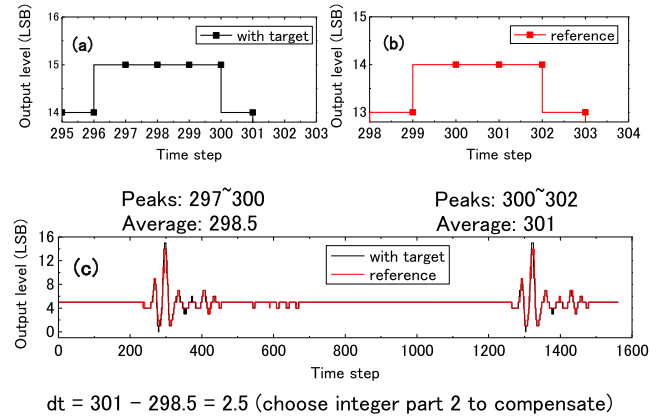dt = 301 − 298.5 = 2.5 (choose integer part 2 to compensate)

FIGURE 17. The signal adjustment procedure from Tx1-Rx5. (a) Peak of 'with target' signal. (b) Peak of 'reference' signal. (c) Alignment of the signals.

An example of adjustment procedure is shown in the Fig. 17. To express the concept clearly, the x axis is shown as time step, where each time step stands for 9.77 ps. It can be seen the two signals are aligned after this process. The original signals and subtracted signals before and after adjustment are shown in Fig. 18. The noise caused by the offset between signals is reduced.

The confocal imaging algorithm is applied to the subtracted signals to reconstruct the image of the breast [46]. The basic concept of the algorithm is to add the reflected signals from the target coherently and the other signals or noise incoherently, to identify the position of the target. The equation to calculate the intensity of a certain position is shown as follows:

$$I(P) = \sum_{i=1}^{Emitter} \sum_{j=1}^{Detector} \int S_{i,j} \left(\frac{\sqrt{\varepsilon_r}(L_1 + L_2)}{c} \right) \qquad (5)$$

where $I(P)$ stands for the intensity of a certain point P and the L_1, L_2 are the distance between the point P and the emitter and detector antenna. ε_r is the assumed relative permittivity of the breast. c is the speed of light.

The imaging result of the detection experiment is shown in Fig. 19. Before the adjustment, as the noise caused by the offset is relatively large, it is hard to recognize the target position from the reconstructed image. After the adjustment, the noise caused by the offset is reduced dramatically and the target can be confirmed in the image. From the imaging results, the estimated position of the target is (20, 25, 20) mm. The target is physically located in (28, 31, 20) mm in the x-y-z coordinate system. The offset error in y direction
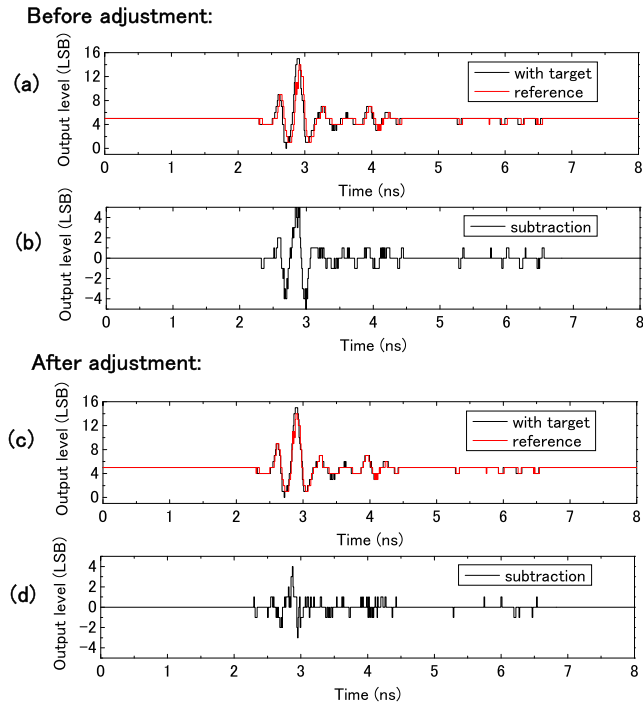
Before adjustment:

After adjustment:

FIGURE 18. Comparison of original and adjusted signals. (a) Raw signals. (b) Subtracted signal. (c) Adjusted signals. (d) Subtracted signal after adjustment.
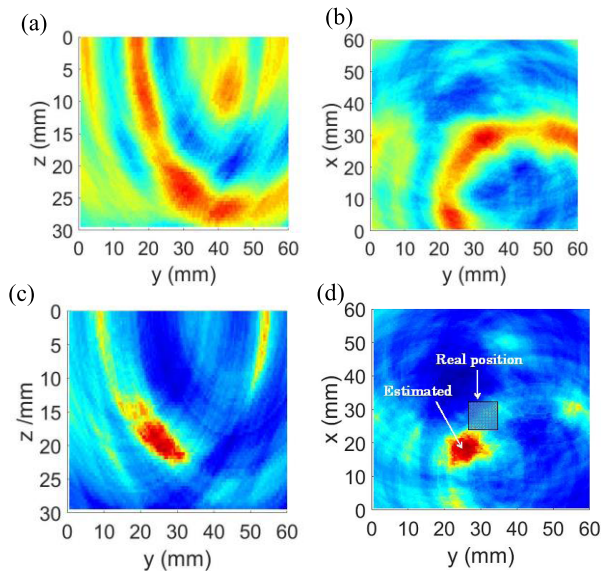

FIGURE 19. Confocal imaging results using row data. (a) y-z cross section before adjustment. (b) x-y cross section before adjustment. (c) y-z cross section after adjustment. (d) x-y cross section after adjustment.

is 6 mm and the error in x direction is 8 mm. This may be caused by the precision of the system.

B. IMAGING FROM 16 TIMES MEASUREMENT DATA

As the ADC is only 4-bit at present, it is sometimes not precise enough to recover the tumor response. However, if the measurement time is increased and then average the signals,

more precise signals can be obtained. Because there are jitters in the sampling timing, the sampled points in the real signal change in different measurements. By averaging the data from several measurements, the effective resolution of the ADC can be improved. In implementation, the signal is transmitted and received at the repetition of 100 MHz. For each Tx-Rx antenna pairs, the sampling and recording operation is taken 16 times. Then the measurement goes for the next Tx-Rx pair. Figure 20(a) shows the measurement data from Tx1-Rx5 which is taken 16 times and Figure 20(b) shows the averaged data. These results demonstrate the averaged signal has a higher resolution.
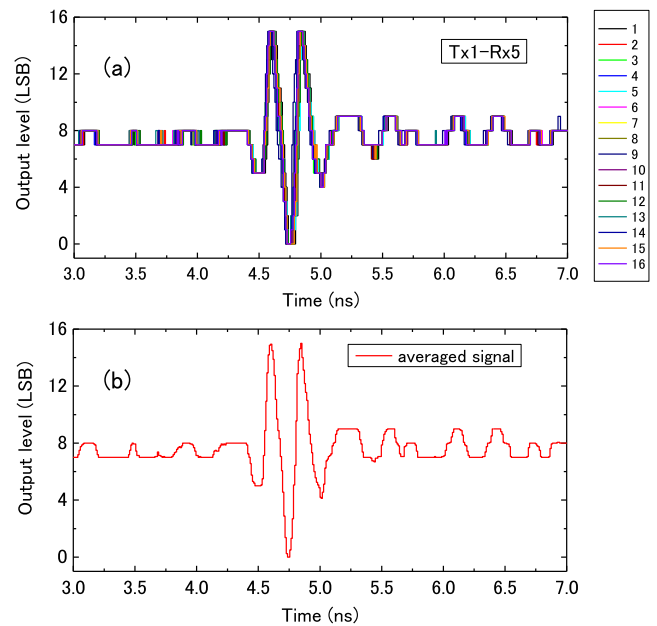
FIGURE 20. The measurement signals from Tx1-Rx5 antenna pair. (a) Raw data for 16 times. (b) Averaged signal.

The image reconstruction is firstly carried out by using the ideal artifacts removal. The reference signals are also measured for 16 times and averaged. Figure 21(a) shows the averaged signals with target and reference signals. The offset between the two signals still exists and the alignment is applied. Figure 21(b) shows the signals after alignment and the subtracted signal is shown in Fig. 21(c).

By use of the averaged signals, the breast image is reconstructed. Figure 22 shows the imaging results. The estimated position of the target is almost the same as the target real position. These results demonstrate that by increasing the measurement time and averaging, the signal accuracy can be improved.

As the ideal artifact removal algorithm is impractical in real case, the averaging artifact removal algorithm is applied to the averaged signals [46]. In implementation, the antenna array is moved in both x and y positions every 20 mm. In total, the experiment is carried out in nine positions. As the relative positions of the antennas are not changed, the waveform of early reflection should be the same.

FIGURE 21. The averaged signals of Tx1-Rx5 antenna pair from 16 measurements. (a) Before adjustment. (b) After adjustment. (c) Subtracted signal.
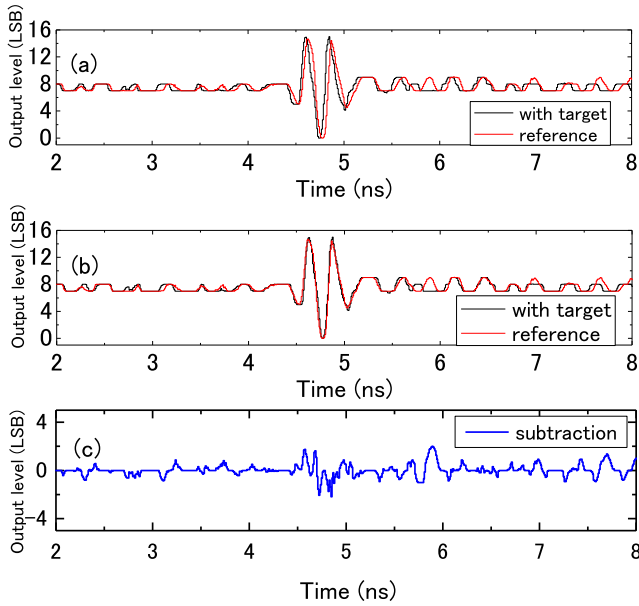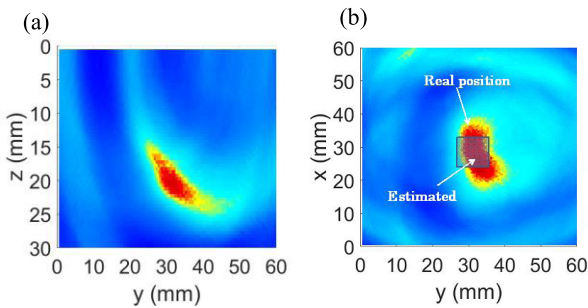

FIGURE 22. Confocal imaging results using averaged data. (a) y-z cross section. (b) x-y cross section.
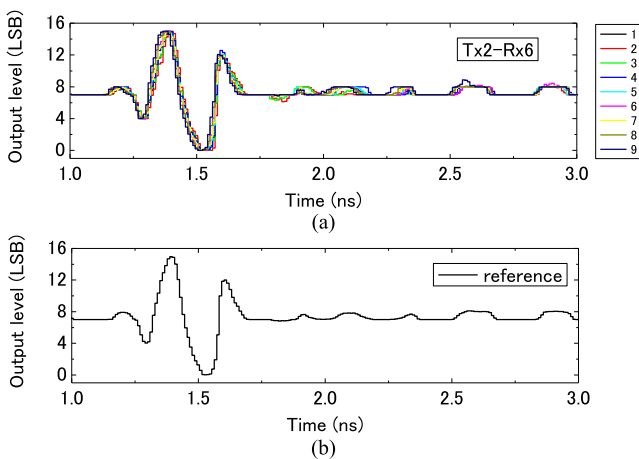

FIGURE 23. The reference signal from Tx2-Rx6 antenna pair. (a) Original signals from nine positions. (b) Reference signal by averaging.

Figure 23(a) shows the waveforms from the Tx2-Rx6 antenna pair in nine positions. There are offsets between signals which are caused by system jitter. To get a reference signal correctly, all the signals are first adjusted to align to the signal from
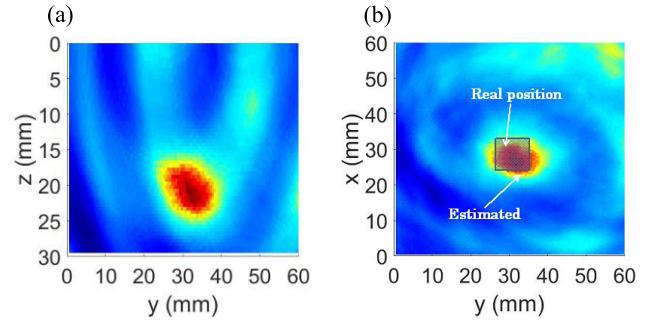

FIGURE 24. Confocal imaging results using averaging artifact removal algorithm. (a) y-z cross section. (b) x-y cross section.

the first position. By taking the average of the nine signals to obtain a reference signal which is shown in Fig. 23(b), this reference signal is employed in image construction in place of the one obtained by the tumor-free experiment. The same process is also applied to other antenna pairs to get a reference signal. The confocal imaging results are shown in the Fig. 24. The estimate position of the tumor is (27, 32, 21) mm, demonstrating the efficacy of the method.

V. CONCLUSION

A CMOS integrated circuits based breast cancer detection system was developed. Compared with the conventional detection systems which employ commercial equipments, the total size of the proposed one is only 45 cm × 30 cm × 14.5 cm. The proposed system is promising in self-examination at home and clinical use in remote areas because of its small size and portability.

The key hardware of the system comprises CMOS UWB signal generation circuits, switching matrix circuits, high-speed sampling circuits and a compact UWB antenna array. During the detection, the GMP signal is generated and guided by the switching matrix to a certain antenna. The reflected signals are recorded by the high-speed sampling circuits. At present, the ADC is 4-bit. However, by increasing measurement times, the effective accuracy of the ADC can be improved. The confocal imaging is employed to test the performance of the system. Both ideal and averaging method are used to remove the artifacts. As there are deviations between measurements, the recorded signals in different cases have offsets. In the ideal case, the offsets between signals with target and tumor-free reference signals are adjusted to get a clear image. In the averaging removal case, the adjustment procedure is applied to align signals from different positions and to generate a reference signal. Imaging results demonstrates the feasibility of the detection system and the efficacy of the method.

REFERENCES

[1] E. C. Fear, S. C. Hagness, P. M. Meaney, M. Okoniewski, and M. A. Stuchly, "Enhancing breast tumor detection with near-field imaging," *IEEE Microw. Mag.*, vol. 3, no. 1, pp. 48–56, Mar. 2002.

[2] R. J. Halter *et al.*, "Real-time electrical impedance variations in women with and without breast cancer," *IEEE Trans. Med. Imag.*, vol. 34, no. 1, pp. 38–48, Jan. 2015.

[3] E. Malone, G. Sato dos Santos, D. Holder, and S. Arridge, "Multifrequency electrical impedance tomography using spectral constraints," *IEEE Trans. Med. Imag.*, vol. 33, no. 2, pp. 340–350, Feb. 2014.

[4] X. Zhang, W. Wang, G. Sze, D. Barber, and C. Chatwin, "An image reconstruction algorithm for 3-D electrical impedance mammography," *IEEE Trans. Med. Imag.*, vol. 33, no. 12, pp. 2223–2241, Dec. 2014.

[5] S. Hong *et al.*, "A 4.9 mΩ-sensitivity mobile electrical impedance tomography IC for early breast-cancer detection system," *IEEE J. Solid-State Circuits*, vol. 50, no. 1, pp. 245–257, Jan. 2015.

[6] M. Lazebnik *et al.*, "A large-scale study of the ultrawideband microwave dielectric properties of normal, benign and malignant breast tissues obtained from cancer surgeries," *Phys. Med. Biol.*, vol. 52, no. 20, pp. 6093–6115, 2007.

[7] M. Lazebnik *et al.*, "A large-scale study of the ultrawideband microwave dielectric properties of normal breast tissue obtained from reduction surgeries," *Phys. Med. Biol.*, vol. 52, no. 10, pp. 2637–2656, 2007.

[8] T. Sugitani *et al.*, "Complex permittivities of breast tumor tissues obtained from cancer surgeries," *Appl. Phys. Lett.*, vol. 104, no. 25, p. 253702, 2014.

[9] E. C. Fear, X. Li, S. C. Hagness, and M. A. Stuchly, "Confocal microwave imaging for breast cancer detection: Localization of tumors in three dimensions," *IEEE Trans. Biomed. Eng.*, vol. 49, no. 8, pp. 812–822, Aug. 2002.

[10] X. Li, E. J. Bond, B. D. Van Veen, and S. C. Hagness, "An overview of ultra-wideband microwave imaging via space-time beamforming for early-stage breast-cancer detection," *IEEE Antennas Propag. Mag.*, vol. 47, no. 1, pp. 19–34, Feb. 2005.

[11] J. D. Shea, P. Kosmas, S. C. Hagness, and B. D. Van Veen, "Three-dimensional microwave imaging of realistic numerical breast phantoms via a multiple-frequency inverse scattering technique," *Med. Phys.*, vol. 37, no. 8, pp. 4210–4226, 2010.

[12] J. D. Shea, B. D. Van Veen, and S. C. Hagness, "A TSVD analysis of microwave inverse scattering for breast imaging," *IEEE Trans. Biomed. Eng.*, vol. 59, no. 4, pp. 936–945, Apr. 2012.

[13] J. M. Sill and E. C. Fear, "Tissue sensing adaptive radar for breast cancer detection—Experimental investigation of simple tumor models," *IEEE Trans. Microw. Theory Techn.*, vol. 53, no. 11, pp. 3312–3319, Nov. 2005.

[14] D. J. Kurrant, E. C. Fear, and D. T. Westwick, "Tumor response estimation in radar-based microwave breast cancer detection," *IEEE Trans. Biomed. Eng.*, vol. 55, no. 12, pp. 2801–2811, Dec. 2008.

[15] J. Bourqui, M. Okoniewski, and E. C. Fear, "Balanced antipodal Vivaldi antenna with dielectric director for near-field microwave imaging," *IEEE Trans. Antennas Propag.*, vol. 58, no. 7, pp. 2318–2326, Jul. 2010.

[16] D. Li, P. M. Meaney, T. Raynolds, S. A. Pendergrass, M. W. Fanning, and K. D. Paulsen, "Parallel-detection microwave spectroscopy system for breast imaging," *Rev. Sci. Instrum.*, vol. 75, no. 7, pp. 2305–2313, 2004.

[17] Q. Fang, P. M. Meaney, and K. D. Paulsen, "Viable three-dimensional medical microwave tomography: Theory and numerical experiments," *IEEE Trans. Antennas Propag.*, vol. 58, no. 2, pp. 449–458, Feb. 2010.

[18] T. M. Grzegorczyk, P. M. Meaney, P. A. Kaufman, R. M. diFlorio-Alexander, and K. D. Paulsen, "Fast 3-D tomographic microwave imaging for breast cancer detection," *IEEE Trans. Med. Imag.*, vol. 31, no. 8, pp. 1584–1592, Aug. 2012.

[19] M. Klemm, I. J. Craddock, J. A. Leendertz, A. Preece, and R. Benjamin, "Radar-based breast cancer detection using a hemispherical antenna array—Experimental results," *IEEE Trans. Antennas Propag.*, vol. 57, no. 6, pp. 1692–1704, Jun. 2009.

[20] D. Gibbins, M. Klemm, I. J. Craddock, J. A. Leendertz, A. Preece, and R. Benjamin, "A comparison of a wide-slot and a stacked patch antenna for the purpose of breast cancer detection," *IEEE Trans. Antennas Propag.*, vol. 58, no. 3, pp. 665–674, Mar. 2010.

[21] S. Kubota *et al.*, "Confocal imaging using ultra wideband antenna array on Si substrates for breast cancer detection," *Jpn. J. Appl. Phys.*, vol. 49, no. 9R, p. 097001, 2010.

[22] X. Li, M. Jalilvand, Y. L. Sit, and T. Zwick, "A compact double-layer on-body matched Bowtie antenna for medical diagnosis," *IEEE Trans. Antennas Propag.*, vol. 62, no. 4, pp. 1808–1816, Apr. 2014.

[23] H. Bahramiabarghouei, E. Porter, A. Santorelli, B. Gosselin, M. Popović, and L. A. Rusch, "Flexible 16 antenna array for microwave breast cancer detection," *IEEE Trans. Biomed. Eng.*, vol. 62, no. 10, pp. 2516–2525, Oct. 2015.

[24] M. Strackx, E. D'Agostino, P. Leroux, and P. Reynaert, "Direct RF subsampling receivers enabling impulse-based UWB signals for breast cancer detection," *IEEE Trans. Circuits Syst. II, Exp. Briefs*, vol. 62, no. 2, pp. 144–148, Feb. 2015.

[25] T. Yin, F. H. Ali, and C. C. Reyes-Aldasoro, "A robust and artifact resistant algorithm of ultrawideband imaging system for breast cancer detection," *IEEE Trans. Biomed. Eng.*, vol. 62, no. 6, pp. 1514–1525, Jun. 2015.

[26] T. U. Gürbüz, B. Aslanyürek, A. Yapar, H. Şahintürk, and I. Akduman, "A nonlinear microwave breast cancer imaging approach through realistic body–breast modeling," *IEEE Trans. Antennas Propag.*, vol. 62, no. 5, pp. 2596–2605, May 2014.

[27] M. A. Elahi, A. Shahzad, M. Glavin, E. Jones, and M. O'Halloran, "Hybrid artifact removal for confocal microwave breast imaging," *IEEE Antennas Wireless Propag. Lett.*, vol. 13, pp. 149–152, 2014.

[28] T. Yin and F. H. Ali, "Adaptive combining via correlation exploration for ultrawideband breast imaging," *IEEE Antennas Wireless Propag. Lett.*, vol. 14, pp. 587–590, 2015.

[29] P. M. Meaney *et al.*, "Microwave imaging for neoadjuvant chemotherapy monitoring: Initial clinical experience," *Breast Cancer Res.*, vol. 15, no. 2, p. R35, 2013.

[30] M. Klemm, J. A. Leendertz, D. Gibbins, I. J. Craddock, A. Preece, and R. Benjamin, "Microwave radar-based breast cancer detection: Imaging in inhomogeneous breast phantoms," *IEEE Antennas Wireless Propag. Lett.*, vol. 8, pp. 1349–1352, 2009.

[31] M. Klemm, J. A. Leendertz, D. Gibbins, I. J. Craddock, A. Preece, and R. Benjamin, "Microwave radar-based differential breast cancer imaging: Imaging in homogeneous breast phantoms and low contrast scenarios," *IEEE Trans. Antennas Propag.*, vol. 58, no. 7, pp. 2337–2344, Jul. 2010.

[32] E. C. Fear, J. Bourqui, C. Curtis, D. Mew, B. Docktor, and C. Romano, "Microwave breast imaging with a monostatic radar-based system: A study of application to patients," *IEEE Trans. Microw. Theory Techn.*, vol. 61, no. 5, pp. 2119–2128, May 2013.

[33] J. Bourqui, J. M. Sill, and E. C. Fear, "A prototype system for measuring microwave frequency reflections from the breast," *J. Biomed. Imag.*, vol. 2012, Jan. 2012, Art. ID 851234.

[34] M. J. Burfeindt, N. Behdad, B. D. Van Veen, and S. C. Hagness, "Quantitative microwave imaging of realistic numerical breast phantoms using an enclosed array of multiband, miniaturized patch antennas," *IEEE Antennas Wireless Propag. Lett.*, vol. 11, pp. 1626–1629, 2012.

[35] A. H. Golnabi, P. M. Meaney, and K. D. Paulsen, "Tomographic microwave imaging with incorporated prior spatial information," *IEEE Trans. Microw. Theory Techn.*, vol. 61, no. 5, pp. 2129–2136, May 2013.

[36] N. R. Epstein, P. M. Meaney, and K. D. Paulsen, "Microwave tomographic imaging utilizing low-profile, rotating, right angle-bent monopole antennas," *Int. J. Antennas Propag.*, vol. 2014, Jun. 2014, Art. ID 431602.

[37] N. R. Epstein, P. M. Meaney, and K. D. Paulsen, "3D parallel-detection microwave tomography for clinical breast imaging," *Rev. Sci. Instrum.*, vol. 85, no. 12, p. 124704, 2014.

[38] T. Kikkawa, P. K. Saha, N. Sasaki, and K. Kimoto, "Gaussian monocycle pulse transmitter using 0.18 μm CMOS technology with on-chip integrated antennas for inter-chip UWB communication," *IEEE J. Solid-State Circuits*, vol. 43, no. 5, pp. 1303–1312, May 2008.

[39] N. Sasaki, K. Kimoto, W. Moriyama, and T. Kikkawa, "A single-chip ultra-wideband receiver with silicon integrated antennas for inter-chip wireless interconnection," *IEEE J. Solid-State Circuits*, vol. 44, no. 2, pp. 382–393, Feb. 2009.

[40] A. Azhari, S. Takumi, S. Kenta, T. Kikkawa, and X. Xiao, "A 17 GHz bandwidth 1.2 mW CMOS switching matrix for UWB breast cancer imaging," in *Proc. IEEE Biomed. Circuits Syst. Conf. (BioCAS)*, Lausanne, Switzerland, Oct. 2014, pp. 109–112.

[41] A. Toya, K. Sogo, N. Sasaki, and T. Kikkawa, "125 mW 102.4 GS/s ultra-high-speed sampling circuit for complementary metal–oxide–semiconductor breast cancer detection system," *Jpn. J. Appl. Phys.*, vol. 52, no. 4S, p. 04CE07, 2013.

[42] A. Toya, N. Sasaki, S. Kubota, and T. Kikkawa, "Confocal imaging system using high-speed sampling circuit and ultra-wideband slot antenna," *Jpn. J. Appl. Phys.*, vol. 50, no. 4S, p. 04DE02, 2011.

[43] S. Kubota, A. Toya, T. Sugitani, and T. Kikkawa, "5-Gb/s and 10-GHz center-frequency Gaussian monocycle pulse transmission using 65-nm logic CMOS with on-chip dipole antenna and high-κ interpose," *IEEE Trans. Compon., Packag., Manuf. Technol.*, vol. 4, no. 7, pp. 1193–1200, Jul. 2014.

[44] T. Sugitani, S. Kubota, M. Hafiz, X. Xiao, and T. Kikkawa, "Three-dimensional confocal imaging for breast cancer detection using CMOS Gaussian monocycle pulse transmitter and 4×4 ultra wideband antenna array with impedance matching layer," *Jpn. J. Appl. Phys.*, vol. 53, no. 4S, p. 04EL03, 2014.

[45] T. Sugitani, S. Kubota, A. Toya, X. Xiao, and T. Kikkawa, "A compact 4×4 planar UWB antenna array for 3-D breast cancer detection," *IEEE Antennas Wireless Propag. Lett.*, vol. 12, pp. 733–736, 2013.

[46] X. Li and S. C. Hagness, "A confocal microwave imaging algorithm for breast cancer detection," *IEEE Microw. Wireless Compon. Lett.*, vol. 11, no. 3, pp. 130–132, Mar. 2001.

[47] M. A. Elahi, M. Glavin, E. Jones, and M. O'Halloran, "Artifact removal algorithms for microwave imaging of the breast," *Prog. Electromagn. Res.*, vol. 141, pp. 185–200, 2013.

[48] H. B. Lim, N. T. T. Nhung, E.-P. Li, and N. D. Thang, "Confocal microwave imaging for breast cancer detection: Delay-multiply-and-sum image reconstruction algorithm," *IEEE Trans. Biomed. Eng.*, vol. 55, no. 6, pp. 1697–1704, Jun. 2008.

JUNICHI SOMEI received the B.S. and M.S. degrees from the Department of Chemical Engineering, Tokushima University, Tokushima, Japan, in 1987. In 1987, he joined the Electronic Components and Devices Division, Sharp Corporation, Osaka, Japan. Since 1987, he has been involved in the development of microwave circuit and low noise block converter. Since 2009, he has also been involved in the development of LED illumination with the Electronic Components and Devices Division, Sharp Corporation, Hiroshima, Japan. His current interests are high frequency system, LED modules, and breast cancer detection.

HANG SONG received the B.S. and M.S. degrees in electronic science and technology from Tianjin University, Tianjin, China, in 2012 and 2015, respectively. He is currently pursuing the Ph.D. degree with Hiroshima University, Hiroshima, Japan.

His research interests are microwave breast cancer detection system, complex permittivities of breast cancer tissues, and antenna design.

HAYATO KONO received the B.S. degree in electrical engineering from Hiroshima University, Hiroshima, Japan, in 2014, where he is currently pursuing the master's degree with the Graduate School of Advanced Sciences of Matter. His research interest is breast cancer detection.

EIJI SUEMATSU received the B.S. and M.S. degrees in geoscience from Kumamoto University, Kumamoto, Japan, in 1985 and 1986, respectively. In 1986, he joined the Central Research Laboratory, Sharp Corporation, Nara, Japan. He was involved in research and development of low-noise FET and monolithic microwave integrated circuits (MMICs). Since 1992, he has been with the ATR Optical and Radio Communications Research Laboratory, Kyoto, Japan, where he has been involved in research on millimeter-wave fiber optic radio systems. Since 1994, he has been involved in research on millimeter-wave MMICs with the Central Research Laboratory, Sharp Corporations. Since 2006, he has also been involved in the development of millimeter-wave and radio frequency devices with the Electronic Components and Devices Division, Sharp Corporation, Hiroshima, Japan. His current interests are microwave radar system and breast cancer detection.

YUJI SEO received the B.S. degree in electrical engineering from Hiroshima University, Hiroshima, Japan, in 2014, where he is currently pursuing the master's degree with the Graduate School of Advanced Sciences of Matter. His research interest is analog integrated circuits design.

YUICHI WATARAI received the B.S. and M.S. degrees from the Department of Electrical and Electronic Engineering, Tokyo Institute of Technology, Tokyo, Japan, in 2010 and 2012, respectively. In 2012, he joined the Electronic Components and Devices Division, Sharp Corporation, Hiroshima, Japan. His current interests are microwave radar system and breast cancer detection.

AFREEN AZHARI received the B.S. and M.S. degrees in electrical and electronics engineering from the Bangladesh University of Engineering and Technology, Dhaka, Bangladesh, in 2001 and 2004, respectively, and the Ph.D. degree in semiconductor electronics and integration science from Hiroshima University, Hiroshima, Japan, in 2011. She is currently a Post-Doctoral Researcher with the Research Institute for Nanodevice and Bio-System, Hiroshima University. Her research interests include CMOS switches for low power radar systems, and RF integrated circuit and system design for wireless and biomedical applications.

TOSHIHIKO OTA received the B.S. degree in communication engineering from Tokai University, Kanagawa, Japan, in 1983. He joined NEC Radio Equipment Engineering, Ltd., in 1983, where he had conducted the development of radar system. Since 1993, he has been with Sharp Takaya Electronic Industry Company, Ltd., where he has directed the development of digital signal processing system for charge-coupled device, and radio frequency system for communication. His current interests are radar sensor and breast cancer detection.

HIROMASA WATANABE received the B.S. and M.S. degrees in electrical engineering and information engineering from Kinki University, Japan, in 2002 and 2004, respectively. He joined Sumitomo Electric Networks Inc., in 2004, where he had conducted the development of communication equipments. Since 2007, he has been with Sharp Takaya Electronic Industry Company, Ltd., where he has conducted the development of wireless communication system. His current interests are analog radio frequency and breast cancer detection.

YOSHINORI HIRAMATSU received the B.S. degree in electrical engineering from Okayama University, Okayama, Japan, in 2005. He joined Sharp Takaya Electronic Industry Company, Ltd., in 2005, where he had conducted the development of antennas and application specified integrated circuits. His current interests are antenna design, analog radio frequency circuit design, and breast cancer detection.

AKIHIRO TOYA received the B.S. degree from the National Institution for Academic Degrees and University Evaluation, Matsue College of Technology, Shimane, Japan, in 2004, and the M.S. and Ph.D. degrees from Hiroshima University, Hiroshima, Japan, in 2006 and 2011, respectively, all in electrical engineering. He joined the Kure National College of Technology in 2013. His current interests are system design, CMOS analog RF circuit design, and breast cancer detection.

XIA XIAO (M'01) received the B.S. degree in physics and the M.S. degree in condensed physics from Tianjin Normal University, Tianjin, China, in 1993 and 1996, respectively, and the Ph.D. degree in electronic and information technology from the Technical University of Chemnitz, Chemnitz, Germany, in 2002. From 2002 to 2003, she was with the MIRAI Project, National Institute of Industrial Science and Technology, Japa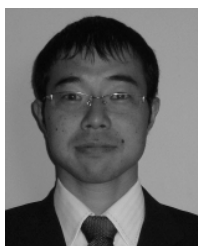n, where she was involved in the low-k/Cu interconnect technology as a Key Researcher. In 2003, she joined the School of Electronic Information Engineering, Tianjin University, where she is currently a Professor. From 2006 to 2007, she was a Visiting Professor with Hiroshima University, Hiroshima, Japan, where she was involved in developing algorithms for ultrawideband imaging for early breast cancer detection.

Her current research interests include advanced algorithms for early breast cancer detection by ultrawideband and non-destructive characterization of film properties by surface acoustic waves.

TAKAMARO KIKKAWA (S'74–M'76–SM'01–F'10) received the B.S. and M.S. degrees in electronic engineering from Shizuoka University, Shizuoka, Japan, in 1974 and 1976, respectively, and the Ph.D. degree in electronic system from the Tokyo Institute of Technology, Tokyo, Japan, in 1994. He joined NEC Corporation, Tokyo, in 1976, where he conducted research and development of interconnect technologies for large scale integrated circuits and dynamic random access memories. From 1983 to 1984, he was a Visiting Scientist with the Massachusetts Institute of Technology, Cambridge, MA, USA, where he conducted research on transistors. In 1998, he joined as a Faculty Member with Hiroshima University, Hiroshima, Japan, where he is currently a Professor with the Graduate School of Advanced Sciences of Matter and the Director of the Research Institute for Nanodevice and Bio Systems. He is also a Councilor of Hiroshima University. From 2001 to 2008, he was appointed as a Senior Research Scientist with the National Institute of Advanced Industrial Science and Technology, Japan, and the Group Leader of Low-k/Cu Interconnect Technology of the MIRAI Project, Japan. His research interests include wireless and wired interconnect technologies, impulse-radio-CMOS transceiver circuits with on-chip antennas, and impulse-radar-based CMOS breast cancer detection system.

Dr. Kikkawa is a fellow of the Japan Society of Applied Physics.

● ● ●